

Analysis of salicylic acid using square-wave voltammetry with pre-concentration by solid phase extraction onto magnetite nanoparticles

Phetlada Sanchayanukun, Prapanee Pengmarerng, and Sasithorn Muncharoen*

Department of Chemistry, Faculty of Science, Burapha University, Chonburi, 20131, Thailand

Abstract

A pencil lead electrode coupling with nano-magnetite adsorption as pre-concentration and extraction in order to analyze salicylic acid (SA) was demonstrated in this work. The optimum conditions for nano-magnetite (Fe_3O_4) preparation by co-precipitation of ferrous/ferric ions were studied. The parameters affecting the shape and size of the nano-magnetite particles such as the types of base, addition rate, temperature, stirring rate and pH were optimized. The morphology was characterized by Fourier transform infrared spectroscopy, energy dispersive X-ray spectroscopy and transmission electron microscopy. The application of nano-magnetite as the solid phase extractor for the square-wave voltammetry (SWV) of SA gave good results.

Keywords: salicylic acid, nano-magnetic particles, solid phase extraction, square-wave voltammetry, pencil lead electrode

Article history: Received 25 April 2018, Accepted 28 February 2019

1. Introduction

Salicylic acid or 2-hydroxybenzoic acid (SA) is a major compound in plants and drugs. It plays a major role in the physical growth processes of plants such as seed regeneration, flowering, heat production, stomatal closure, membrane permeability and ion absorption. In addition, SA has important antipathogen activities in plants. It is also used in medicine as an oral and external drug. It can be used as antipyretic, antithrombotic, anti-inflammatory and analgesic drugs. In addition to this it is used in skin cosmetics including products to remove corns, calluses and warts. SA is clearly very useful in various applications but it may cause illnesses such as allergic reactions, dehydration, dizziness, deafness, reduced pulse force and rapid breathing in the case of excessive usage [1-4]. It is therefore necessary to determine the quantity of SA required to control product quality and minimize these side effects [5].

Recently, nano-materials including magnetite (Fe_3O_4) have been used in numerous applications such as catalysis [6], drug delivery [7] and contrast agents in magnetic resonance imaging (MRI) [8, 9]. They have also been used for separations [10], extractions including analyses using magnetic field assistance and as the adsorbent material for removal of metals from waste [10]. Various methods for nano-magnetite synthesis have been developed. These include sol-gel reactions [11, 12], thermal decomposition [13, 14], sonochemical synthesis [15] and co-precipitation [16-18]. The co-precipitation of

ferrous/ferric compounds in alkaline solution is the most common method for nano-magnetite synthesis. This is due to its simplicity in providing small particles with diameters of 10 nm or less with high surface areas. The particles produced by this method are particularly suitable for application as the adsorbent material for separation or extraction.

SA analysis using visible spectrometry based on monitoring of the purple complex of SA-Fe(III) is a method that is common [19]. The color of this complex, however, is interfered with alcohol and phenol groups, which effects the visible spectrometric signals received. Other analytical approaches used for determination of SA such as spectrofluorometry [20], capillary electrophoresis [21, 22], flow injection analysis [23] and chromatography [24] have been developed. Of particular interest are electrochemical techniques which have been demonstrated to have certain advantages such as accuracy, economy, and rapidity [25, 26]. However, the sensitivity and selectivity of these methods are still problems.

This paper outlines the first time a pencil lead electrode has been used as an inexpensive working electrode [27] for demonstration of SA analysis coupling to the pre-concentration method based on adsorption onto the nano-magnetite particles. The particles were detected using a square-wave voltammetric method (SWV). In addition, the method for preparation of

* Corresponding author; e-mail: muncharoen@go.buu.ac.th

suitable nano-magnetite particles used as the adsorbent in solid phase extraction was validated.

2. Materials and Methods

2.1 Reagents and materials

All of the reagents used were analytical grade (AR-grade). FeCl₃ (Fluka, Switzerland), FeCl₂·4H₂O (Panreac, Barcelona), 25 wt% ammonia solution (NH₄OH) (QRec, New Zealand) and HCl (Loba chemie, India) were used for the Fe₃O₄ synthesis. For the SA analysis, various concentrations of SA (C₇H₆O₃) (Rankem, India) were prepared in a 1 M ammonium buffer (NH₃/NH₄Cl) at pH 8.0. Deionized water was used throughout.

Electrochemical experiments were performed using a potentiostat (PGSTAT20, Metrohm, Switzerland). A 3 electrodes system was used; a pencil-lead electrode as the working electrode (household working electrode) [28], Ag/AgCl electrode (reference electrode) and a platinum wire electrode (auxiliary electrode).

2.2 SA analysis using the pencil lead electrode

A HB pencil lead with 0.7 mm diameter coated with epoxy resin was used as the household working electrode in this work [28]. Measurements were carried out using cyclic voltammetry (CV) with a potential range of -0.8 to +1.5 V at a scan rate of 20 mV·s⁻¹. Before each run, the working electrode was carefully polished with Al₂O₃ powder (0.3 μm, Metrohm) and rinsed with deionized water before being dried with a soft cloth.

2.3 Preparation of nano-magnetite particles

A co-precipitation method was used for the synthesis of nano-magnetite particles (Fe₃O₄) [16]. The appropriate amounts of FeCl₃ and FeCl₂·4H₂O with molar ratio 2:1 were dissolved in 2M HCl with mechanical stirring and the color of the resulting solution was observed as being wine-red. The precipitating agent (base solution) was added to the Fe(III)/Fe(II) solution using a peristaltic pump with constant stirring at a specified temperature for 120 min. The black precipitate was allowed to settle and was then separated using a magnetic field. The precipitate was washed with deionized water to remove all of the impurity ions until the pH of wash solution was neutral. Finally, the Fe₃O₄ particles were dried in an oven at 120°C for 120 min. The chemical equation for the formation of magnetite is as follows [29].



2.4 Characterization of the nano-magnetite particles

The nano-magnetite particles were initially characterized by Fourier transform infrared spectroscopy (FT-IR) (Spectrum System 2000: Perkin Elmer) in the wavelength range of 400-4000 cm⁻¹ for identifi-

cation functional group. The synthesized particles were mixed with dried KBr (Merck) at the ratio of nano-magnetite: KBr = 1:100. Then the mixed particles were compressed into a pellet. Additionally, a transmission electron microscope (TEM) (Tecnai20, Philips) and energy dispersive X-ray spectroscopy (EDX) were used for morphology and element analysis of the nano-magnetite particles. The diameter of the particles was measured from TEM micrographs by Insinooritoimisto Rimppi Oy, Finland (SemAfore 5.21).

2.5 Pre-concentration of SA using nano-magnetite

The method for pre-concentration of SA using nano-magnetite as the adsorbent for solid phase extraction was adapted from Parham and Rahbar [34]. For testing the adsorption and desorption of SA by the particles, 0.25 g of the synthesized nanoparticles were added to 100.0 mL of a solution containing 0.05-3.50 mM of SA with 0.20 mL of 0.1 M FeCl₃ (to form a Fe(III)-SA complex). The solution was mixed for 30 min and then the nano-magnetite particles were collected using a magnet. The particles were washed with 2.0 mL of 1.0 M NaOH and stirred for 120 min in order to desorb the SA. The supernatant solution was collected and diluted with 1 M ammonia buffer (pH 8.0) in a 10 mL volumetric flask. The total amount of SA in the solution was determined by use of the square wave voltammetric technique (SWV).

The SWV was performed by a potentiostat (PGSTAT20, Metrohm, Switzerland) using the pencil-lead household working electrode, Ag/AgCl reference electrode and the platinum wire auxiliary electrode. The SWV voltammograms were recorded by applying a potential range of -0.8 to +1.5 V with a frequency of 25 Hz, a step potential of 5 mV and an amplitude of 20 mV.

3. Result and Discussion

3.1 SA analysis using the pencil lead electrode

Electrochemical behaviours of the household pencil lead electrode for analysis of SA were tested using CV (as above-mentioned). It was found that SA only showed an irreversible anodic peak as shown in Figure 1. The anodic potential was found to be at approximately +1.10 V. This corresponded to previous work [1, 25-26]. It could therefore be stated that the household pencil lead electrode has the potential to determine SA concentration. The key advantage of this electrode is that it is cheap however its main weakness is its low sensitivity (Figure 1). Thus, nano-magnetite was used as an adsorbent material for solid phase extraction in order to improve the sensitivity of the overall proposed method.

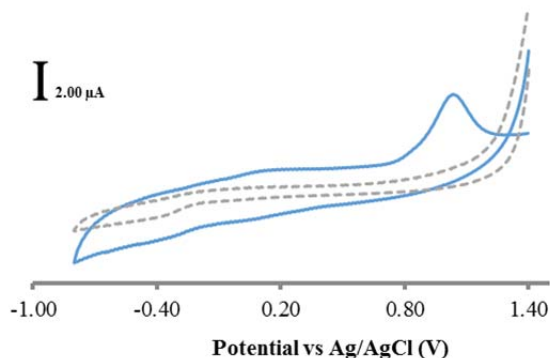


Figure 1 Cyclic voltammogram of SA solution concentration at 4 mM (solid line) and electrolyte solution: buffer (dash line). Condition; scan potential -0.8 to 1.4 V at scan rate 20 mV/s

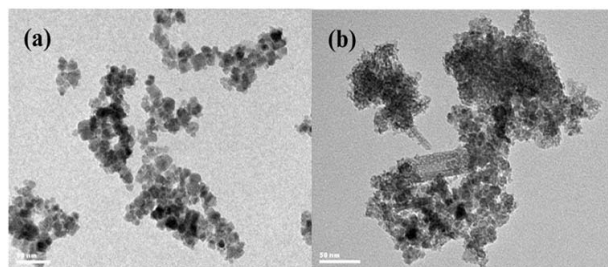


Figure 2 TEM images of nano-magnetite particles synthesized using (a) NH_4OH and (b) NaOH as precipitating agents with reaction temperature, addition and mixing rates were 50°C , $15 \text{ mL} \cdot \text{min}^{-1}$ and 1225 rpm , respectively

3.2 Optimization of experimental parameters for preparation of nano-magnetite particles

1) Types of basic solutions and addition rate

Solutions with concentrations of 0.7 M NH_4OH and NaOH were studied. The results showed that the types of basic solution had an effect on the size and shape of the particles. The average diameters of the particles produced from NH_4OH and NaOH were 8 ± 2 and $4 \pm 2 \text{ nm}$, respectively. Although the precipitates synthesized from NaOH gave smaller size than these from NH_4OH , it was observed that the synthesized nano-magnetite particles produced from NaOH were highly aggregated (Figure 2). Subsequently, 0.7 M NH_4OH was selected as the precipitating agent to produce the most suitable nano-magnetite particles for this research.

Increasing the addition rate of 0.7 M NH_4OH solution decreased the particles size obtained as illustrated in Figure 3(a). This result agrees with Valenzuela et al. [18] and consistent with that predicted by nucleation-crystal growth theory. However, it was found that the particles size did not decrease much

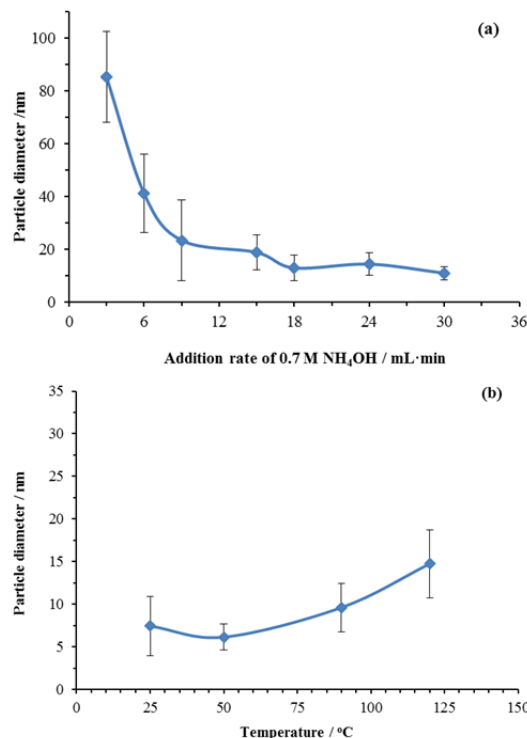


Figure 3 Average diameter of magnetite particles generated by (a) various addition rate of 0.7 M NH_4OH and (b) various reaction temperatures

above an addition rate of $15 \text{ mL} \cdot \text{min}^{-1}$. This addition rate was therefore selected for further experiments.

2) Temperature

Experiments were conducted at temperatures between 26 - 120°C using 0.7 M NH_4OH and an additional rate at $15 \text{ mL} \cdot \text{min}^{-1}$. The effect of the reaction temperature on particle diameter is shown in Figure 3(b). The results showed that the particle size of magnetite increased with increasing temperature because the particle growth was accelerated by the heat [17]. A reaction temperature of 50°C was selected for further syntheses that should yield particles of about $7 \pm 2 \text{ nm}$ in diameter because it produced particles with the smallest size and the smallest standard deviation.

3) Mixing rate

The effect of mixing or stirring rate (470 - $1,225 \text{ rpm}$) on the particle diameter of the magnetite particles produced was studied. It was observed that the average size of the synthesized particles only differed slightly when the rate was changed. A mixing rate at $1,225 \text{ rpm}$ ($6 \pm 2 \text{ nm}$) was therefore chosen for further experiments because it produced particles with the smallest standard deviation.

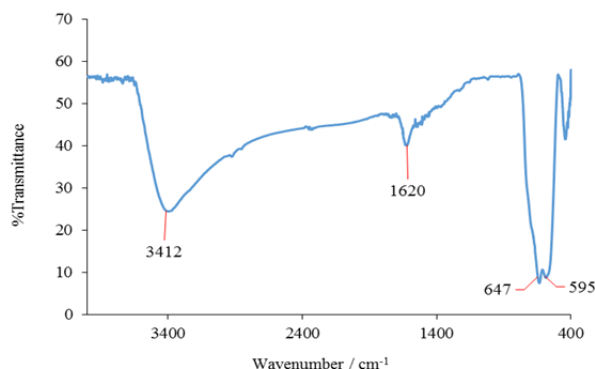


Figure 4 FT-IR spectrum of the synthesized nano-magnetite particles

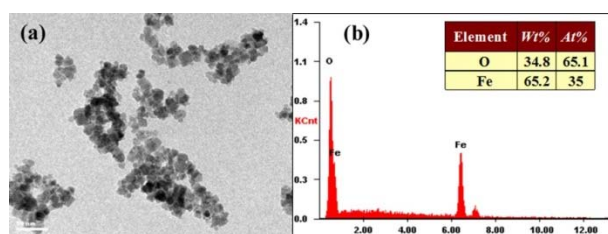


Figure 5 (a) TEM image and (b) EDX spectrum of the synthesized nano-magnetite particles

4) pH of mixed solution

Mixed solutions of FeCl_3 , $\text{FeCl}_2 \cdot 4\text{H}_2\text{O}$ and NH_4OH at various pH levels were studied. The results showed that the sizes of nano-magnetite particles slightly decreased on increasing pH of the mixed solution (pH 8 and 11). A pH of 6 was also investigated and results showed that the particles did not form at this pH. This confirmed that particles do not form at acidic pH levels as found by Mascolo [29]. A pH of 11 was therefore selected for subsequent work.

3.3 Characterization of nano-magnetite particles

The FT-IR spectrum of the synthesized particles is shown in Figure 4. The strong absorbance peaks at 647 cm^{-1} and 595 cm^{-1} correspond to the Fe-O bond in stretching vibration mode [30-32]. The peak at 3412 cm^{-1} is the characteristic of the OH bond in stretching vibration mode. It could be caused from hydrolyzation on the surface of Fe_3O_4 particles. In addition, the peak at 1620 cm^{-1} confirmed the existence of Fe-O bonds [32].

The element analysis was studied by EDX. It was confirmed that the synthesized particles contained only Fe and O elements. The spectrum indicated that surface molar ratio of Fe and O were 65-67% and 33-35%, respectively. Additionally, the spherical shape of the nano-magnetite particles was illustrated by TEM image. It gave average diameter in the range of $7 \pm 2 \text{ nm}$ as shown in Figure 5. Photographs of the synthesized nanoparticles are shown in Figure 6.

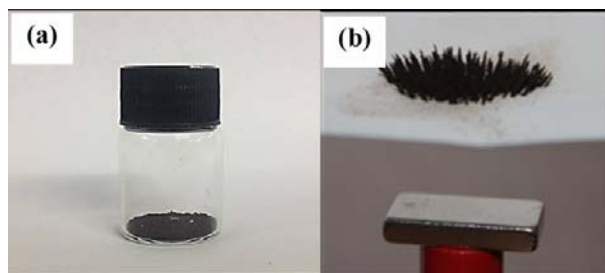


Figure 6 (a) Photographs of the synthesized nanoparticles and (b) a side view of the spiking nanoparticles in the presence of a magnet placed underneath a filter paper

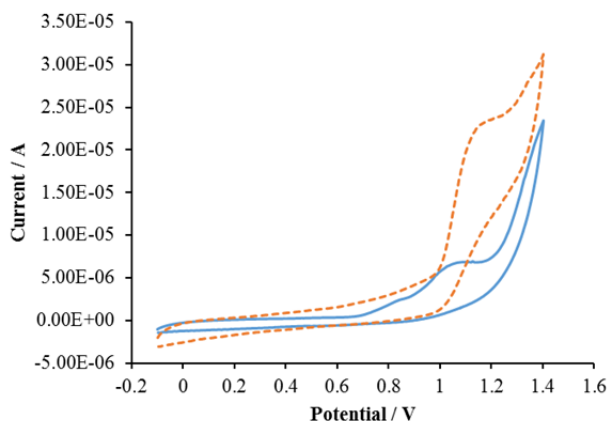


Figure 7 Cyclic voltammograms of 4 mM SA (solid line) and desorbed SA (dash line) in ammonium buffer (pH 8)

3.4 Pre-concentration of SA using nano-magnetite

To investigate the feasibility of the pencil lead working electrode to determine SA, CV was applied. Figure 7 presents cyclic voltammograms of SA. The solid line (—) and dash line (---) in Figure 7 represents results from standard solution of SA and SA desorbed from nano-magnetite particles, respectively. As shown in the Figure 7, the CV was carried out in the potential range from -0.8 to 1.4 V. At a potential of around 1.04 V, both peaks are illustrated only as the oxidation peaks of SA. These results are in agreement with previous studies of SA [1, 33]. It was confirmed that the eluted solution by using NaOH following the experimental scheme consisted only of desorbed SA.

The selectivity of SA analysis for this method, which based on adsorption of SA-Fe(III) complex was tested. This was done by comparing the anodic current of SA between the addition and non addition of Fe(III) into the sample/standard following the topic of pre-concentration of SA using nano-magnetite. The obtained results showed that the adsorption of SA was not significant without adding Fe(III) into the solution as shown in Figure 8. It was found that SA adsorption on

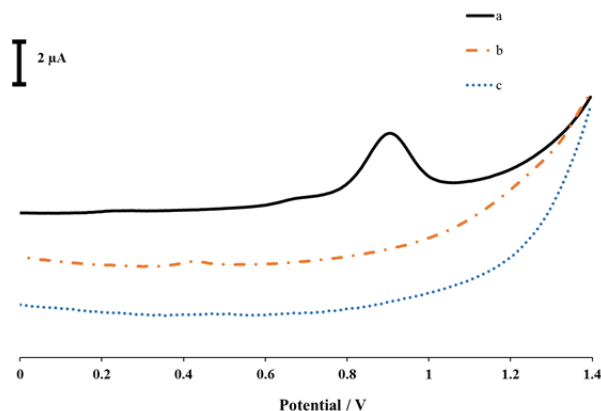


Figure 8 Square wave voltammograms of SA adsorbed onto nano-magnetite particles with (a) addition of FeCl_3 , (b) without addition of FeCl_3 and (c) buffer

the magnetite nanoparticles occurred via the complex of SA-Fe(III). This result agreed with Parham [34].

3.5 Method validation

Thirteen concentrations of SA containing 0.05-3.50 mM were used for a linearity range study. The calibration graph was plotted using the anodic current of SA (y-axis) versus SA standard concentrations (x-axis). This graph was found to be linear over the concentration range of 0.05-3.50 mM with a correlation coefficient (r^2) of 0.9988. This calibration graph is described by the calibration equation $y = 3.0073x + 0.0284$. The validity of concentrations of SA on the peak current in ammonium buffer (pH 8.0) using SWV is shown in Figure 9.

The limit of quantification (LOQ) and limit of detection (LOD) were also investigated. LOQ was established for the lowest concentration at which the analyte could be quantified. Here the LOQ was determined and calculated using the lowest concentration of analyte in the calibration graph following the method described in Miller & Miller [35]. By definition, LOD is the lowest concentration of the analyte that can be detected. In this study, LOQ and LOD were 0.05 mM and 0.02 mM, respectively. The accuracy of the method was determined by analyzing 10.0 mM solution of SA 10 times under the optimal conditions. The accuracy for SA analysis was found to be 5.5%. This was within the 6% limit stated by AOAC 2012 [36].

3.6 Recovery

Extraction recoveries were studied in the range of 0.02-.20 mM original concentration of SA. After the pre-concentration step using the magnetite nanoparticles, the results of percentage recovery were found to be in the range of 83-96% as shown in Table 1. These values are consistent with AOAC 2012 [36]. Thus, the proposed method has an acceptable performance for the analysis of SA.

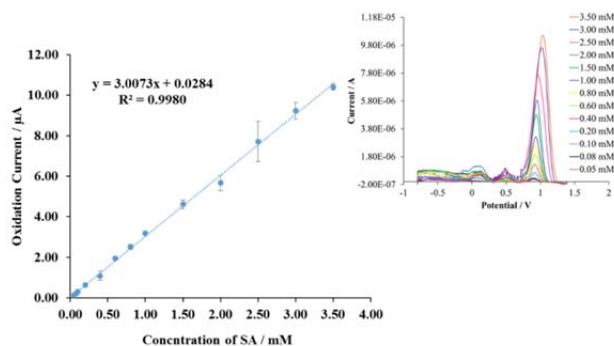


Figure 9 (a) Calibration graph of anodic current of SA versus concentration of SA standard and (inset) SWV-voltammograms for oxidation of SA at different concentrations 0.05-3.50 mM in the potential range from -0.8 to 1.4 V, step potential 50 mV, amplitude 1.0 V

Table 1 Recovery percentage of desorbed SA using the proposed method

Original SA (mM)	Pre-concentrated SA (mM)	Detected SA (mM)	Percentage recovery (%)
0.02	0.20	0.17 ± 0.02	83
0.05	0.50	0.46 ± 0.03	93
0.08	0.80	0.76 ± 0.14	96
0.10	1.00	0.96 ± 0.11	96
0.20	2.00	1.88 ± 0.32	94

4. Conclusions

One of the key utilities of nano-magnetite particles is to act as an adsorbent to increase the selectivity and sensitivity for SA determination. This method was illustrated and analysed in this article. The optimum synthesis conditions to produce the particles with diameter <10 nm were reported. The proposed synthetic particle shapes and sizes were characterized by TEM images and the composition and element were confirmed by FT-IR and EDX spectroscopy. This proposed method was found to be simple and fast for SA analysis using SWV. In addition, this method was applied for SA analysis in a drug for the treatment of dermatitis and it gave satisfactorily results. The method therefore has the potential for the further applications with real samples in pharmaceutical and other products.

Acknowledgements

This work was financially supported by the Research Grant of Burapha University through National Research Council of Thailand (Grant no. 60/2559 and 233/2561) and the Center of Excellence for Innovation in Chemistry (PERCH-CIC). Moreover, we express thanks to Ms. Chonticha Tongtumachart and Ms. Juthamas Buntungtang for their preliminary study. Finally, we thank Dr. Ronald Beckett for useful suggestions on the manuscript.

References

- [1] Torriero AAJ, Luco JM, Sereno L, Raba J. Voltammetric determination of salicylic acid in pharmaceuticals formulations of acetylsalicylic acid. *Talanta*. 2004; **62** (2): 247–254.
- [2] Petrek J, Havel L, Petrlova J, Adam V, Potesil D, Babula P, Kizek R. Analysis of salicylic acid in willow barks and branches by an electrochemical method. **Published in Russian in Fiziologiya Rastenii**. 2007; **54** (4): 623–628.
- [3] Baxter GJ, Lawrence JR, Graham AB, Wiles AB, Paterson JR. Identification and determination of salicylic acid and salicyluric acid in urine of people not taking salicylate drugs. *Annals of Clinical Biochemistry*. 2002; **39** (1): 50–55.
- [4] Arshadi M, Mousavinia F, Abdolmaleki MK, Amiri MJ, Khalafi-Nezhad A. Removal of salicylic acid as an emerging contaminant by a polar nano-dendritic adsorbent from aqueous media. *Journal of Colloid and Interface Science*. 2017; **493** (1): 138–149.
- [5] US Department of Health and Human Services, Food and Drug Administration. Center for Drug Evaluation and Research (CDER) and Center for Veterinary Medicine (CVM). **Database of FDA guidance for industry**. Bioanalytical Method Validation; 2001. [cited 25 July 2017]. Available from <https://www.fda.gov/downloads/Drugs/Guidance/ucm070107.pdf>.
- [6] Gao Y, Wang G, Huang H, Hu J, Shah SM, Su X. Fluorometric method for the determination of hydrogen peroxide and glucose with Fe₃O₄ as catalyst. *Talanta*. 2011; **85** (2): 1075–1080.
- [7] Wang G, Chen G, Wei Z, Dong X, Qi M. (2013). Multifunctional Fe₃O₄/grapheme oxide nanocomposites for magnetic resonance imaging and drug delivery. *Materials Chemistry and Physics*. 2013; **141** (2): 997–1004.
- [8] Zhu H, Tao J, Wang W, Zhou Y, Li P, Li Z, Yan K, Wu S, Yeung KWK, Xu Z, Xu H, Chu PK. Magnetic, fluorescent, and thermo-responsive Fe₃O₄/rare earth incorporated poly (St-NIPAM) core-shell colloidal nanoparticles in multimodal optical/magnetic resonance imaging probes. *Biomaterials*. 2013; **34** (9): 2296–2306.
- [9] Song X, Luo X, Zhang Q, Zhu A, Ji L, Yan C. Preparation and characterization of biofunctionalized chitosan/Fe₃O₄ magnetic nanoparticles for application in liver magnetic resonance imaging. *Journal of Magnetism and Magnetic Materials*. 2015; **388** (1): 116–122.
- [10] Lin Z, Zhang Z, Li Y, Deng Y. Magnetic nano-Fe₃O₄ stabilized Pickering emulsion liquid membrane for selective extraction and separation. *Chemical Engineering Journal*. 2016; **288** (1): 305–311.
- [11] Lemine OM, Omri K, Zhang B, El ML, Sajjeddine M, Alyamani A, Bououdina M. Sol–gel synthesis of 8 nm magnetite (Fe₃O₄) nanoparticles and their magnetic properties. *Superlattices and Microstructures*. 2012; **52** (4) 793–799.
- [12] Cui H, Liu Y, Ren W. Structure switch between α -Fe₂O₃, γ -Fe₂O₃ and Fe₃O₄ during the large scale and low temperature sol-gel synthesis of nearly mono-dispersed iron oxide nanoparticles. *Advanced Powder Technology*. 2013; **24** (1): 93–97.
- [13] OanhVTK, Tran DL, Le TL, Pham DV, Pham HN, Le NTH, Do HM, Nguyen XP. Synthesis of high-magnetization and monodisperse Fe₃O₄ nanoparticles via thermal decomposition. *Materials Chemistry and Physics*. 2015; **163** (1): 537–544.
- [14] Amara D, Felner I, Nowik I, Margel S. Synthesis and characterization of Fe and Fe₃O₄ nanoparticles by thermal decomposition of triiron dodecacarbonyl. *Colloids and Surfaces A: Physicochemical and Engineering Aspects*. 2009; **339** (3): 106–110.
- [15] Vijayakumar R, Koltypin Y, Felner I, Gedanken A. Sonochemical synthesis and characterization of pure nanometer-sized Fe₃O₄ particles. *Materials Science and Engineering A*. 2000; **286** (1): 101–105.
- [16] Berger P, Adelman NB, Beckman KJ, Campbell DJ, Ellis AB. Preparation and properties of an aqueous ferrofluid. *Journal of Chemical Education*. 1999; **76** (7): 943–948.
- [17] Petcharoen K, Sirivat A. Synthesis and characterization of magnetite nanoparticles via the chemical co-precipitation method. *Materials Science and Engineering B*. 2012; **177** (1): 421–427.
- [18] Valenzuela R, Fuentes MC, Parra C, Baeza J, Duran N, Sharma SK, Knobel M, Freer J. Influence of stirring velocity on the synthesis of magnetite nanoparticles (Fe₃O₄) by the co-precipitation method. *Journal of Alloys and Compound*. 2009; **488** (1): 227–231.
- [19] Mitchell-Koch JT, Reid KR, Meyerhoff ME. Salicylate detection by complexation with Iron (III) and optical absorbance spectroscopy an undergraduate quantitative analysis experiment. *Journal of Chemical Education*. 2008; **85** (12): 1658–1659.
- [20] Street KW, Schenk GH. Spectrofluorometric determination of acetylsalicylic acid, salicylamide, and salicylic acid as an impurity in pharmaceutical preparations. *Journal of Pharmaceutical Sciences*. 1981; **70** (8): 641–646.
- [21] Frank W, Colyer CL. Using Capillary Electrophoresis to determine the purity of acetylsalicylic acid synthesized in the undergraduate laboratory. *Journal of Chemical Education*. 2001; **78** (11): 1525–1527.
- [22] Sekar R, Prasad PR, Vairamani M. Determination of acetylsalicylic acid and related substances in

- pharmaceutical preparations and bulk drugs by capillary electrophoresis. **Indian Journal of Chemical Technology**. 2003; **10** (1): 603-606.
- [23] Pereira AV, Aniceto C, Fatibello-Filho O. Flow injection spectrophotometric determination of acetylsalicylic acid in tablets after on-line microwave-assisted alkaline hydrolysis. **Analyst**. 1998; **123** (1): 1011-1015.
- [24] Fogel J, Epstein P, Chen P. Simultaneous high-performance liquid chromatography assay of acetylsalicylic acid and salicylic acid in film-coated aspirin tablets. **Journal of Chromatography A**. 1984; **317** (1): 507-511.
- [25] Jinwoo P, Eun C. Electrochemical behavior and determination of salicylic acid at carbon-fiber electrodes. **Electrochimica Acta**. 2016; **194** (1): 346-356.
- [26] Ribeiroa CDL, Santosa JGM, Souza JRd, Pereira-da-Silva MA, Paterno LG. Electrochemical oxidation of salicylic acid at ITO substrates modified with layer-by-layer films of carbon nanotubes and iron oxide nanoparticles. **Journal of Electroanalytical Chemistry**. 2017; **805** (1): 53-59.
- [27] Preechaworapun A, Lertsuwunpisal P, Tangkuaram T. Differential pulse anodic stripping voltammetry for lead (II) cadmium (II) and zinc (II) Analysis on a low cost pencil carbon electrode. **Journal of Thai Interdisciplinary Research**. 2016; **11** (4): 1-7.
- [28] Ditikulchaimongkol J, Muncharoen S. Design and fabrication of a simple electrode for undergraduates to study the quantitative electrochemical analysis. **In Proceedings of Pure and Applied Chemistry International Conference 2012 (PACCON 2012)**. 2012; 325-328.
- [29] Mascolo MC, Pei Y, Ring TA. Room temperature co-precipitation synthesis of magnetite nanoparticles in a large pH window with different bases. **Materials**. 2013; **6** (12): 5549-5567.
- [30] Tahmasebi E, Yamini Y, Moradi M, Esrafil A. Polythiophene-coated Fe₃O₄ superparamagnetic nanocomposite: synthesis and application as a new sorbent for solid-phase extraction. **Analytica Chimica Acta**. 2013; **770** (1): 68-74.
- [31] Lu W, Shen Y, Xie A, Zhang W. Green synthesis and characterization of superparamagnetic Fe₃O₄ nanoparticles. **Journal of Magnetism and Magnetic Materials**. 2010; **322** (13): 1828-1833.
- [32] Cai Y, Shen Y, Xie A, Li S, Wang X. Green synthesis of soya bean sprouts mediated superparamagnetic Fe₃O₄ nanoparticles. **Journal of Magnetism and Magnetic Materials**. 2010; **322** (19): 2938-2943.
- [33] Ghoreishi SM, Kashani FZ, Khoobi A, Enhessari M. Fabrication of a nickel titanate nanoceramic modified electrode for electrochemical studies and detection of salicylic acid. **Journal of Molecular Liquids**. 2015; **211** (1): 970-980.
- [34] Parham H, Rahbar N. Solid phase extraction-spectrophotometric determination of salicylic acid using magnetic iron oxide nanoparticles as extractor. **Journal of Pharmaceutical and Biomedical Analysis**, 2009; **50** (1): 58-63.
- [35] Miller JN, Miller JC. (2010). **Statistics and chemometrics for analytical chemistry**. 6th ed, UK: Gosport Publishing; 2010, pp.124-127.
- [36] Association of official Analytical Chemist (AOAC). **Data base of AOAC International Methods Committee Guidelines for Validation of Microbiological Methods for Food and Environmental Surfaces**; 2002 [cited 30 July 2017]. Available from: https://www.aoac.org/aoac_prod_imis/AOAC_DocsStandardsDevelopment/SLV_Guidelines_Dietary_Supplements.pdf.